

# REGISTRATION OF CONTOURS OF BRAIN STRUCTURES THROUGH A HEAT-KERNEL REPRESENTATION OF SHAPE

Jonathan Bates<sup>1</sup>, Ying Wang<sup>2</sup>, Xiuwen Liu<sup>2</sup>, Washington Mio<sup>1</sup>

<sup>1</sup> Department of Mathematics, Florida State University, Tallahassee, FL 32306-4510

<sup>2</sup> Department of Computer Science, Florida State University, Tallahassee, FL 32306-4530

## ABSTRACT

We develop an algorithm for the registration of surfaces representing the contours of various subcortical structures of the human brain. We employ a scale-space representation of shape based on the heat kernel, which only depends on the intrinsic geometry of the surfaces. The multi-scale representation is used in conjunction with the non-linear Iterative Closest Point algorithm based on thin-plate-spline warps to establish point correspondences between shapes. The method is applied to the registration of the contours of four subcortical structures: the hippocampus, caudate nucleus, putamen, and third ventricle.

**Index Terms**— Shape registration, spectral representation, heat-kernel representation, surface registration.

## 1. INTRODUCTION

We present a surface registration method based on a scale-space representation of shape derived from the heat kernel. The registration of surfaces that delineate the contours of various brain sub-structures such as the hippocampus, thalamus, caudate nucleus, putamen, and ventricles is a theme that emerges in many problems in neuroimaging. Establishing natural point correspondences between surfaces is an essential step in the analysis and comparison of the brain anatomy of individuals or groups, for example, to characterize regional morphological differences associated with a particular population or disorder. Often, surfaces are represented as meshes, and the registration of two surfaces  $S_1$  and  $S_2$ , represented by meshes  $M_1$  and  $M_2$ , is posed as the problem of assigning to each vertex of  $M_1$  a point in  $M_2$ .

The Iterative Closest Point (ICP) algorithm [1] is one of the early shape registration methods. In ICP, a vertex of  $M_1$  is initially assigned to the closest point in  $M_2$ . Then, a transformation is applied to warp  $M_2$  and “optimally” align it with  $M_1$  under the estimated point correspondences, and the process is iterated. If points that are expected to match are initially close enough, ICP performs well, but otherwise the al-

gorithm may not produce meaningful shape correspondences. In [2], Chui and Rangarajan developed a variant that uses soft assignment to describe correspondences between point clouds and thin-plate-spline (TPS) warps [3] for non-rigid alignment. However, even under TPS warps, closeness of points in 3D space may not effectively account for the geometry of the surfaces, especially at fine scales. To address these issues, several studies replaced the original mesh in 3D space with a (low-dimensional) spectral representation derived from the affinity of all pairs of vertices as measured by the geodesic distances between them [4, 5, 6]. This type of representation is more robust to non-linear deformations as it only depends on the intrinsic geometry of the surfaces. One of the virtues of such a representation is that, under appropriate conditions, points that are expected to correspond map to close points in the spectral domain, whereupon an ICP-type strategy is more likely to produce correct matches. However, the calculation of the affinity matrix of a high-resolution mesh can be costly, and so limits the algorithm’s applicability.

We propose use of a scale-space representation of surfaces based on the heat kernel that can be computed much more efficiently. The heat-kernel representation (HKR) is expressed in terms of the eigenvalues and eigenfunctions of the Laplace-Beltrami operator  $\Delta$ . We use HKRs in conjunction with a variant of the matching techniques of [2], based on soft assignment and TPS warps, for the registration of closed surfaces. The multi-resolution representation allows us to take a coarse-to-fine approach to registration and to suppress noise in the registration process. We apply the method to the surface of the hippocampus, caudate nucleus, putamen, and third ventricle. The data used was provided by the Center for Morphometric Analysis at Massachusetts General Hospital and is available at <http://www.cma.mgh.harvard.edu/ibsr/>. A different registration method that uses the Laplace-Beltrami operator has been developed by Shi et al. [7].

The heat-kernel representation is introduced in Section 2, and its discrete analogue is discussed in Section 3, including the computation of the eigenvalues and eigenvectors of  $\Delta$ . In Section 4, we outline the registration technique, and several examples are given in Section 5. We conclude with a summary and brief discussion.

This research was supported in part by NSF grants DMS-0713012 and CCF-0514743, and NIH Roadmap for Medical Research grant U54 RR021813.

## 2. HEAT-KERNEL REPRESENTATION

Let  $S$  be a closed smooth surface in 3D space. The Laplace-Beltrami operator  $\Delta$  on  $S$  is a generalization of the usual Laplacian of functions on planar domains and is given by

$$\Delta f = \operatorname{div}(\nabla f), \quad (1)$$

where  $\operatorname{div}$  and  $\nabla$  are the Riemannian divergence and gradient operators, respectively. Equivalently,  $\Delta f = *d*d$ , where  $d$  denotes the exterior derivative and  $*$  is the Hodge star operator. The heat kernel on  $S$  may be expressed as

$$K(x, y, t) = \sum_{i=0}^{\infty} e^{-\lambda_i t} \phi_i(x) \phi_i(y), \quad (2)$$

where  $x, y \in S$  and  $t > 0$  [8]. The scalars  $\lambda_i \geq 0$  are the eigenvalues of  $-\Delta$  and  $\{\phi_i, i \geq 0\}$  is a complete set of orthonormal eigenfunctions with respect to the inner product  $\langle f, g \rangle = \int_S f(x)g(x) d\sigma$ , where  $d\sigma$  is the area element of  $S$ . Thus,  $\Delta\phi_i = -\lambda_i\phi_i$ . As usual, we order the eigenvalues so that  $\lambda_i \leq \lambda_{i+1}$ . Henceforth, we assume that  $S$  is connected, which implies  $\lambda_0 = 0$  and  $\lambda_i > 0$  for  $i \geq 1$ . The eigenfunctions of  $\lambda_0 = 0$  are the constant functions on  $S$ . Generically, the eigenvalues have multiplicity 1, in which case the eigenfunctions  $\phi_i$  are uniquely determined up to sign. The mappings  $x \in S \mapsto K(x, \cdot, t)$ ,  $t > 0$ , give a scale-space representation of the surface  $S$  in function space.

Let  $p$  be a positive integer. The coordinates of  $K(x, \cdot, t)$  with respect to the orthonormal family  $\{\phi_1, \dots, \phi_p\}$  yield a  $p$ -dimensional scale-space representation of  $S$ , namely,

$$x \mapsto [e^{-\lambda_1 t} \phi_1(x) \quad \dots \quad e^{-\lambda_p t} \phi_p(x)]^T, \quad (3)$$

where  $T$  denotes transposition. Note that we exclude the constant eigenfunction  $\phi_0$  from the representation. Because of the sign ambiguity in the choice of  $\phi_i$ , there are  $2^p$  different representations of this type. We resolve this ambiguity in the registration process.

If we scale a shape by a factor  $r > 0$ , the eigenvalues of  $\Delta$  divide by  $r^2$ . Likewise, for the eigenfunctions to remain orthonormal, they must be divided by  $r$ . For shape registration, we normalize scale by  $r = \sqrt{\lambda_1}$  so that the eigenvalues of  $-\Delta$  become  $\lambda_i/\lambda_1$ , and (3) changes to

$$x \mapsto \frac{1}{\sqrt{\lambda_1}} [e^{-t} \phi_1(x) \quad \dots \quad e^{-\lambda_p t/\lambda_1} \phi_p(x)]^T. \quad (4)$$

## 3. DISCRETE REPRESENTATION

We assume that all surfaces are realized as closed triangle meshes. We now describe the finite-difference discretization of the Laplace-Beltrami operator (cf. [9]). Let  $V = \{v_1, \dots, v_n\}$  be the vertex set of a surface mesh, where the vertices are ordered arbitrarily. For each  $i$ , let  $R(i)$  be

the index set of the 1-ring of  $v_i$ , that is, of the vertices adjacent to  $v_i$ . If  $j \in R(i)$ , let  $\ell_{ij}$  be the length of the edge  $e_{ij} = (v_i, v_j)$ . We denote the length of the 1-cell  $e_{ij}^*$  dual to  $e_{ij}$  by  $\ell_{ij}^*$ , and the area of the 2-cell  $T_i^*$  dual to  $v_i$  by  $A_i$  (see Fig. 1). A function  $f: S \rightarrow \mathbb{R}$  is discretized over the vertex

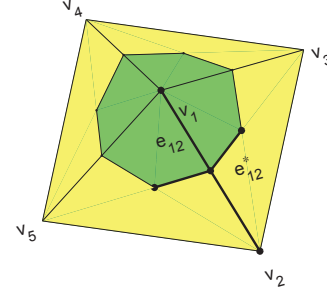


Fig. 1. Example of a dual cell of a triangulation.

set  $V$  and represented by the  $n$ -vector  $f = [f_1 \dots f_n]^T$ , where  $f_j = f(v_j)$ . With these conventions, the  $i$ th entry of  $\Delta f$  is

$$(\Delta f)_i = \Delta f(v_i) = \frac{1}{A_i} \sum_{j \in R(i)} \frac{f_j - f_i}{\ell_{ij}} \ell_{ij}^*. \quad (5)$$

This is a geometric discretization of the divergence of the gradient. The term  $(f_j - f_i)/\ell_{ij}$  is the directional derivative of  $f$  along the oriented edge  $(v_i, v_j)$ . The summation estimates the total outward flux of the gradient field  $\nabla f$  across the boundary of the 2-cell  $T_i^*$ , and the full expression represents the flux density over the 2-cell  $T_i^*$ .

The natural discretization of the  $\mathbb{L}^2$  inner product over the geometric mesh is

$$\langle f, g \rangle = \sum_{i=1}^n (f_i g_i) A_i, \quad (6)$$

not the usual dot product  $(f \cdot g)$ . One can show that  $-\Delta$  is self-adjoint with respect to  $\langle \cdot, \cdot \rangle$ , with eigenvalues  $0 = \lambda_0 < \lambda_1 \leq \dots \leq \lambda_n$ . The matrix of a self-adjoint operator with respect to any orthonormal basis is symmetric. If  $E_i$ ,  $1 \leq i \leq n$ , is the canonical basis of  $\mathbb{R}^n$ , it is easy to check that  $E_i/\sqrt{A_i}$  is orthonormal with respect to  $\langle \cdot, \cdot \rangle$ . The  $(i, j)$ -entry of the symmetric matrix  $B$  that represents the operator  $-\Delta$  with respect to this orthonormal basis is

$$b_{ij} = \begin{cases} \frac{1}{A_i} \sum_{k \in R(i)} \frac{\ell_{ik}^*}{\ell_{ik}}, & \text{if } i = j; \\ \frac{-1}{\sqrt{A_i A_j}} \frac{\ell_{ij}^*}{\ell_{ij}}, & \text{if } j \in R(i); \\ 0, & \text{otherwise.} \end{cases} \quad (7)$$

The matrix  $B$  is sparse, so the eigenvalues  $\lambda_1, \dots, \lambda_p$  and a corresponding set of orthonormal eigenvectors  $u_1, \dots, u_p$

(with respect to the usual Euclidean dot product) can be computed efficiently with Krylov subspace methods for  $p$  small. The eigenvalues of  $-\Delta$  are the same as those of  $B$ . If we write  $u_i = [u_{i1} \dots u_{in}]^T$ , then the corresponding orthonormal eigenfunctions of  $-\Delta$  with respect to (6) are

$$\phi_i = \left[ \frac{u_{i1}}{\sqrt{A_1}} \dots \frac{u_{in}}{\sqrt{A_n}} \right]^T. \quad (8)$$

Fig. 2 (a) shows the level sets of  $\phi_1, \phi_2$ , and  $\phi_3$  of a putaminal surface computed with this method. Notice how the level sets slice the surface in complementary directions, resembling an  $(x, y, z)$ -system.

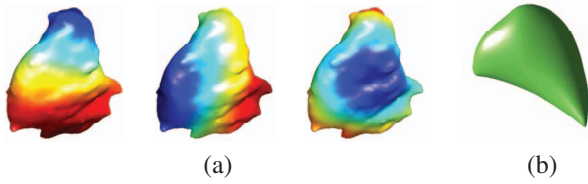


**Fig. 2.** (a) Plots of the first 3 eigenfunctions of a putaminal surface; (b) a 3D heat-kernel representation of the surface.

The discrete analogue of the normalized representation (4) is defined on the vertex set by

$$v_j \mapsto \frac{1}{\sqrt{\lambda_1}} \left[ \frac{e^{-t}}{\sqrt{A_j}} u_{1j} \dots \frac{e^{-\lambda_p t / \lambda_1}}{\sqrt{A_j}} u_{pj} \right]^T. \quad (9)$$

We write (9) as the  $j$ th column of a matrix  $Q(t)$ , whose  $(i, j)$ -entry is

$$q_{ij} = \frac{e^{-\lambda_i t / \lambda_1}}{\sqrt{\lambda_1 A_j}} u_{ij}. \quad (10)$$

Given a mesh  $M$ , we refer to the  $p \times n$  matrix  $Q(t)$  as its  $p$ -dimensional HKR at time  $t$ .  $Q(t)$  may be viewed as an analogue of the reduced affinity matrices of [4, 5, 6]. Fig. 2 (b) shows a normalized 3-dimensional representation of a putaminal surface computed with the method just described.

#### 4. SHAPE REGISTRATION

Let  $M_1$  and  $M_2$  be meshes with vertex sets  $V_1 = \{v_1, \dots, v_n\}$  and  $V_2 = \{w_1, \dots, w_m\}$ , where  $n$  and  $m$  may be different and the orderings of the vertices are arbitrary. For each  $t > 0$ , let  $Q_1(t)$  and  $Q_2(t)$  be the associated  $p$ -dimensional HKRs.

We adapt methods of [2] to register surfaces in spectral coordinates, representing homologous surfaces originally given in Talairach coordinates. There are three principal differences in the optimization process: (i) the initial steps of the shape matching focus on a coarse sampling of the vertex set of  $M_1$ ; (ii) we use a heat-kernel representation, except for the initial vertex assignment done in Talairach coordinates; (iii) at the fine-resolution level, the refinements of the correspondence

iterate over regions of the mesh to achieve computational efficiency for even high-resolution meshes. Now, we expand on these three aspects of the registration algorithm.

To begin, we construct a coarse subset  $V^*$  of the vertex set of  $M_1$  by decomposing  $M_1$  into several approximately uniform disjoint regions  $R_\ell$  and selecting a vertex lying near the “center” of each region, as illustrated in Fig. 3. We call such



**Fig. 3.** Decomposition of a hippocampal surface into regions.

a vertex the center of  $R_\ell$ . In the original 3D representation, after centering and scaling the vertex sets, we assign to each vertex of  $V^*$  the closest vertex of  $M_2$ . For general shapes, this may not produce meaningful correspondences. However, this procedure is effective for brain surfaces in Talairach coordinates – this claim is supported by our experimental results. In spectral space, we compute the  $p \times p$  orthogonal matrix  $U$  that optimally aligns the shapes with respect to the given correspondences and replace  $Q_2(t)$  with  $UQ_2(t)$ . The calculation of  $U$  is identical to that in Procrustes alignment of shapes [10]. Note that a sign change of an eigenfunction corresponds to a reflection in the spectral representation so that the estimation of  $U$  includes the decision of best choices of signs. We iterate the process to refine the correspondences over  $V^*$ , now in spectral space, using TPS mappings to warp the HKR of  $M_1$ .

Next, we proceed to soft assignments with TPS warps for all vertices of  $M_1$ , not just those in  $V^*$ . To keep the calculations manageable, we refine the assignments iteratively over each region  $R_\ell$ . As we already have constructed a coarse alignment, given a vertex  $v \in R_\ell$ , we only allow for (soft) matches comprising vertices in a neighborhood of the vertex of  $M_2$  closest to  $v$  with respect to the current warp. As the process is iterated, we shrink the size of the neighborhood until it is reduced to the set of vertices within the 1-ring of the closest vertex to  $v$ . We also gradually increase the number  $p$  of eigenvectors used in the HKR to capture geometry at finer scales.

#### 5. EXPERIMENTS

We test our method on meshes, downloaded from the Center for Morphometric Analysis, representing four brain substructures, namely, the hippocampus, putamen, caudate nucleus, and third ventricle. The number of vertices in these meshes falls in the 1000–3000 range. For each structure, a

target mesh is selected from among those in the collection (shown as the leftmost shape of each group in Fig. 4), and the other surfaces are registered with it. In these experiments, either a 3- or 4-dimensional HKR is invoked in the coarse alignment, depending on the shape, and the same HKR is used for the first iteration of the fine-resolution-level alignment. The dimension of HKR increments by one per iteration and the registration algorithm terminates with an HKR of dimension at most 7. We add one dimension to the HKR per iteration to keep the refinement of the correspondence gradual. The use of low-dimensional representations makes the registration algorithm robust to fine-scale differences. The value of the time parameter for each HKR is selected empirically and is the same over all shapes and HKRs considered. The approximate size of the regions  $R_\ell$  vary with structure, according to the mesh size. Some results obtained with the proposed registration method are shown in Fig. 4. Each registration completed in under ten minutes on a 3GHz Intel Xeon MP processor.

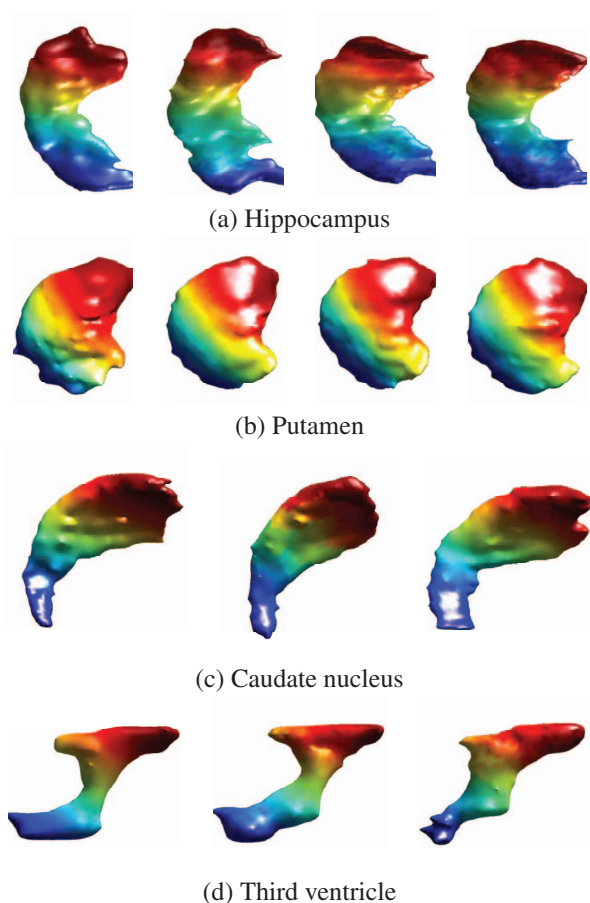


**Fig. 4.** Surface registration with a heat-kernel representation.

## 6. SUMMARY AND DISCUSSION

We employed a scale-space representation of shape based on the heat kernel to develop an algorithm for the registration of contour surfaces of various brain structures as encountered in neuroimaging. The shape representation can be computed efficiently via the eigenvalues and eigenvectors of the Laplace-Beltrami operator and only depends on the intrinsic geometry of a surface. The representation is used in conjunction with the non-linear ICP algorithm based on TPS warps for shape registration. The efficacy of the method has been demonstrated on several experiments with subcortical structures of the human brain. The selection of parameter values for specific types of shapes, as well as refinements of the algorithm using surface diffeomorphisms to establish point correspondences shall be investigated in future work.

## 7. REFERENCES

- [1] P. J. Besl and N. D. McKay, "A method for registration of 3D shapes," *IEEE Trans. Pattern Anal. Mach. Intell.*, vol. 14, no. 2, pp. 239–256, 1992.
- [2] H. Chui and A. Rangarajan, "A new point matching algorithm for non-rigid registration," *Comput. Vis. Image Underst.*, vol. 89, no. 2-3, pp. 114–141, 2003.
- [3] G. Wahba, *Spline Models for Observational Data*, SIAM, Philadelphia, PA, 1990.
- [4] V. Jain, H. Zhang, and O. van Kaick, "Non-rigid spectral correspondence of triangle meshes," *Internat. J. Shape Modeling*, vol. 13, no. 1, pp. 101–124, 2007.
- [5] D. Mateus, F. Cuzzolin, R. Horaud, and E. Boyer, "Articulated shape matching by robust alignment of embedded representations," in *ICCV*, 2007, pp. 1–8.
- [6] X. Liu, A. Donate, M. Jemison, and W. Mio, "Kernel functions for robust 3D surface registration with spectral embeddings," in *ICPR*, 2008.
- [7] Y. Shi, R. Lai, K. Kern, N. Sicotte, I. Dinov, and A. W. Toga, "Harmonic surface mapping with laplace-beltrami eigenmaps," in *MICCAI*, 2008.
- [8] S. Rosenberg, *The Laplacian on a Riemannian Manifold*, Cambridge University Press, 1997.
- [9] M. Desbrun, A. Hirani, M. Leok, and J. Marsden, "Discrete exterior calculus," arXiv:math/0508341v2, 2005.
- [10] D. G. Kendall, "Shape manifolds, Procrustean metrics and complex projective spaces," *Bull. London Math. Soc.*, vol. 16, pp. 81–121, 1984.